



Analysis on the junction point's stress located at considering fluid-solid coupling effects for support arm under different wall thickness

Authors: Zhi-jin Zhou^{1, a}, Zhi Yang^{1, b}, Zhaohui WANG^{2, c}, Xiong Chen^{1, d}, Wang Zhao^{3, e}

¹School of Mechanical & Electrical Engineering; Hunan University of Science and Technology; Xiangtan 411201, China;

²Hunan Provincial Key Laboratory of Health Maintenance for Mechanical Equipment; Hunan University of Science and Technology; Xiangtan 411201, China;

³National Key Lab of Deepsea Mineral Resources Development and Utilization, Changsha Research Institute of Mining and Metallurgy, Changsha 410012, China

^azjzhou@hnust.edu.cn, ^b254198705@qq.com, ^c307327000@qq.com, ^d393915182@qq.com

Abstract:

Fluid-structure interaction has a significant effect on stresses in the hinge point because of the impact of ocean currents to the pipeline. Aimed to support arms for deep-sea mining, numerical analysis method and the finite element software ADINA were adopted to analyze the pipeline structure - external fluid mutual coupling effect on stress at the hinge point. The results were shown that: (1) In the case of different wall thickness, the stress changes of the entire pipeline is relatively small, stress located mainly these places close to the junction in the pipelines, the maximum stress exists at the upper connection; (2) With wall thickness of the support pipe increasing, the maximum stress decreases, and when wall thicknesses

changed from 9.5mm to 28.7mm interval 2.4mm ,the maximum stress value decreased 19.3%, 15.9%, 13.5%, 11.7%, 10.3%, 9.2%, 8.3%, 7.6% ;(3) With wall thickness increasing, the minimum stress value also reduced, and a minimum stress values decreased 19.9%, 14.0%, 5%, 14.6%, 28.7%, 15.9%, 8.6%, 2.7%,respectively .

Key words:Support arm; Fluid–structure interaction; Different wall thickness; Stress

Introduction

Fluid-structure interaction problems and general multi-physics problems are often too complex and difficult to analyze and solve, so they would be completed by experimental or numerical simulation method.Because of the Computational Fluid Dynamics and computational structural dynamics field study obtain great progress, these achievements make the fluid-structure interaction numerical simulation is completed.

At the same time, the way of Newton-Raphson and Fixed point iteration can be used to solve the problem which is involve in Fluid-structure interaction.In view of Newton-Raphson iteration method the monolithic ^{[1] [2] [3]} and partition ^{[4] [5]} method has been widely used.We can use the Newton-Raphson method to solve the nonlinear fluid equations and structural equation. The problem of the system lacking the knowledge of Jacobi matrix iteration method can be solved by the iterative linear equations within the Newton- Raphson. Besides, it can use the product finite difference of vector Jacobi to approximatie.

As we all know, Newton-Raphson method can not only work out the state flow and structural problems in the whole liquid and solid domain, but also may be applied to the FSI device problem of multi-degree freedom system on the situation of interface location unknown.This domain decompose and condense into subspace FSI problem error ^[6].Therefore, the FSI problem with the unknown location of the interface can be transformed into the problem of finding roots or fixed point .

Using the Newton-Raphson iterative interface Newton - Raphson method may be able to find the answers, such as the Jacobi approximation linear physical model ^{[7] [8]}.In the coupling iteration process , using the least squares model coupling the black boxes and the Newton Falla comparable to reverse approach for solving the domain of fluid and structure ^[9].This

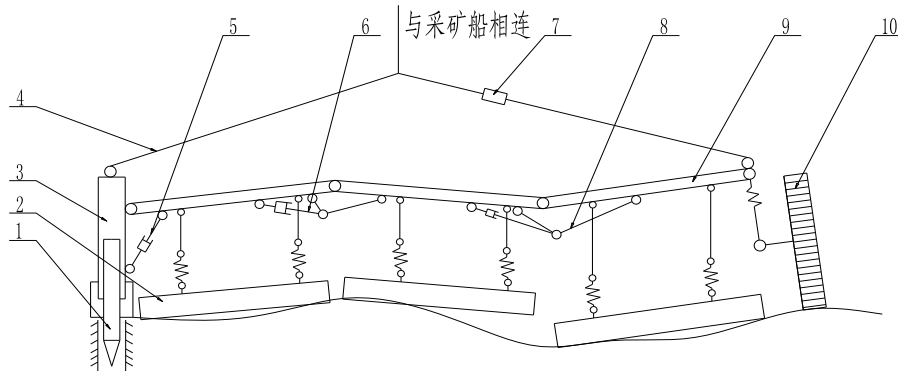
technique is based on the interface of quasi Newton least square model, and re-expresses FSI problem as the Jacobian matrix approximation technique of an unknown equation which is in the condition of system interface location and interface stress distribution. The system solves the Gauss - Seidel type and the fluid and structure solving the Jacobian matrix block quasi-Newton iterative approximation least squares model^[10]. The fixed point problem can be solved by fixed point iteration which is also known as the Gauss - Seidel iteration^[6]. It means that the fluid and structural issues have been resolved, until the change is less than the convergence criterion. However, the convergence speed is slow, especially in times of the interaction between the fluid and structural strong, such as High density fluid, Structure proportion or incompressible fluid. It adapts to the fixed point iteration convergence based on previously iteration, which can be stabilized and accelerated by the fastest descent relaxation factors and Aitken relaxation.

If the interaction between the fluid and the structure is weak, it only needs a fixed point iteration in each time step. This was so-called staggered or loosely coupled method does not enforce the balance of the fluid structure interface within a time step, but they apply to the structure simulation with the structure of the heavy and fairly rigid. Doing some part of research analysis the stability of the interaction segmentation algorithm used to simulate the fluid-structure stability^{[11][12]}.

Putting forward the Pivot arm - outrigger composite collection agencies, as shown in figure 1. The collection agency was mainly consisted of the outrigger, pivot arm, holder, buoyancy wheel and cylinder. Pivot arm rotating around the outrigger, double lower end of the Cantilever using hinge to connect, the upper using the cylinder support and adjustment. The wheel worked as the support and enhance the buoyancy effect. The mining head was driven by the screw on Pivot arm.

During the Bracket walls (hollow tube) rotating around outrigger, it was an elastomer and affected by the internal and external fluids. The role of the fluid caused the pipe wall deformation or movement, which would change the morphology of the flow field in turn, thus changing the state of the fluid flow, and so affect the movement and deformation of the pipe. Under the support of the different constraints, this interaction between the pipe and fluid would produce a variety of different patterns of fluid-structure interaction phenomena^[3], that is the strongly nonlinear coupling between the pipe and the fluid. Scholars in the past mostly paid more attention on the level of transmission, fixed support, elastic support

(multi-point) pipeline studies [4-7],negligence the study on one end of the pipe vibration, not to mention the research on the dynamic characteristics of the pipeline in the fluid-structure interaction effect of the transport process with the heave compensation device hinged support case ^{[13][14]}.



1 - outrigger ; 2 - bracket; 3 - pumping the pump; 4 - cylinder; 5 - duct; 6 - Extractive head; 7 - propulsion units; 8 - screw; 9 - Roller (buoyancy material); 10 – seafloor

Fig.1 Cantilever - outrigger composite mining mechanism

Stress Analysis in the connection points

When bracket piping around the legs rotate, as in the marine environment, the support pipe will inevitably be affected by the role of the waves and currents. Besides, it would also bear its own gravity, buoyancy and internal pulp. There is no really ideal fluid in nature. For the viscosity coefficient μ (coefficient of dynamic viscosity and was also known as a first coefficient of viscosity) of the fluid, its basic equation:

The Mass conservation equation:

$$\frac{\partial \rho}{\partial t} + \text{div}(\rho u) = 0 \quad (1)$$

The Momentum conservation equation:

$$\frac{\partial}{\partial t}(\rho u) + \text{div}(\rho u \otimes u - P) = \rho F \quad (2)$$

Among of them $P = \{p_{ij}\}$.

$$p_{ij} = -p\delta_{ij} + \mu\left(\frac{\partial u_i}{\partial x_j} + \frac{\partial u_j}{\partial x_i}\right) + \mu'\text{div}u\delta_{ij} \quad (3)$$

Among of them $\mu' = \lambda + \frac{2}{3}\mu$ It is called the Expansion viscosity coefficient or the Second viscosity coefficient.

The Energy conservation equation:

$$\frac{\partial}{\partial t} \left(\rho e + \frac{1}{2} \rho u^2 \right) + \text{div} \left(\left(\rho e + \frac{1}{2} \rho u^2 \right) u - p u \right) = \text{div}(k \text{grad} T) + \rho F \cdot u \quad (4)$$

k is the Thermal conductivity coefficient. Above of the equations constitute a viscous hydrodynamic equations. Density is constant for viscous incompressible viscous fluid, take

$$\rho \equiv 1000 \text{Kg} / \text{m}^3$$

Therefor $\text{div} u = 0$ (5)

Momentum conservation equation can be changed to the following equation.

$$\frac{\partial u_i}{\partial t} + \sum_{k=1}^3 u_k \frac{\partial u_i}{\partial x_k} - \mu \Delta u_i + \frac{\partial p}{\partial x_i} = F_i \quad (6)$$

The above conservation of energy and momentum conservation equations are the three-dimensional Navier-Stokes equations of incompressible viscous fluid, which is short as the NS equations.

Considering the seawater is non-ideal fluid and the relative speed of the lifting system can not be ignored, seawater are taken as a viscous fluid in the calculation .We get knowledge from the fluid mechanics that viscous fluid will generate the flow around detached phenomenon of the boundary layer separation when the viscous fluid flow around is not streamlined objects. Obviously, when the shape of Support pipe was a cylinder, it was adverse streamlined objects. The flow around phenomenon of the viscous fluid is different when it flow around the adverse streamlined objects at the different Reynolds. We can get the following form fluid dynamics.

$$\text{Re} = \frac{\rho v d}{\eta} \quad (7)$$

Among of them : ρ ——the density of seawater; v ——the flow rate of seawater; d ——the viscosity coefficient of seawater (It have some relationship with seawater temperature.)

Seawater flow rate in the deep-sea mining process will change, small changes in other parameters can be ignored. When the support pipe work in seawater, the relative velocity of the currents and Support pipe work as the following.

$$V = V_c + V_h \quad (8)$$

Among of them : V_c ——the speed of the mining ship; V_h ——at a depth of ocean currents speed; the solving formula for ocean current speed:

$$V_h = (V_a - V_b)e^{(-hH)} + V_b \quad (9)$$

Among of them : e ——natural constants; V_h ——the flow rate of the water depth h ; V_a ——the speed of the sea currents; V_b ——the speed of the deep ocean currents; h —— the calculated depth of Pipeline; H ——water depth.

The main resistance of the support pipe flow around is composed by the frictional resistance and the pressure drag ^[16].

$$F_D = F_f + F_p \quad (10)$$

$$F_f = \int_A \tau_0 \sin\theta dA \quad (11)$$

$$F_p = \int_A p \sin\theta dA \quad (12)$$

Among of them : A -the total surface area of the object; θ -The normals of the object surface differential area dA and the direction of flow's angle.

Frictional resistance and pressure drag can be expressed as the kinetic energy of the flow in the unit volume with a particular area of the product, coupled with a drag coefficient.

$$F_f = C_f \frac{\rho U_0^2}{2} A_f \quad (13)$$

$$F_p = C_p \frac{\rho U_0^2}{2} A_p \quad (14)$$

Among of them : C_f ——the frictional resistance coefficient; C_p ——the pressure drag coefficient; A_f ——the Shear stress area; A_p ——the facing the flow projected area of the Support pipe perpendicular to flow velocity.

In the working process of the lifting system, not only will the ocean currents and the mining ship towage produce drag force, but also the waves will produce drag force. This force is closely related to the density of seawater, the geometry of wave size and shape and the Support pipe. Here is the formula.

$$f = \frac{1}{2} \rho_w C_D D |u - y'| (u - y') + \rho_w C_M \frac{\pi D^2}{4} a_y - \rho_w (C_M - 1) \frac{\pi D^2}{4} y'' \quad (15)$$

Among of them : u — the horizontal velocity of the water points; C_D — drag coefficient; a_y — the horizontal acceleration of the water points; C_M — inertial force coefficient; D — Support pipe diameter; y — Support pipe lateral offset; ρ_w — the density of seawater.

Stress analysis at the hinge

Pipe with different wall thickness, the junction points of pipeline generate different stress values in the same flow impact speed. Although we can find the foreign pipeline wall thickness range data, we need to analyze it to find its own rules. After information search, we can get the data that the abroad pipeline wall thickness selected range of 9.2mm-28.7mm, the simulation analysis of pipe wall thickness in the range. Selecting a wall thickness of 9.5mm, 11.9mm, 14.3mm, 16.7mm, 19.1mm, 21.5mm, 23.9mm, 26.3mm, 28.7 mm to analyze the stress changes, the velocity in the external flow field is 1.8 m / s, the speed in the internal flow field is 2m / s, in the case of different wall thicknesses obtained effects such as stress cloud shown in Figures 2 and 3.

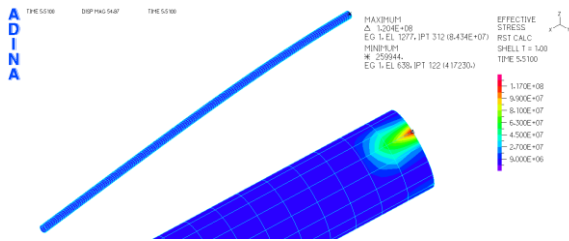


Fig.2 Wall thickness is 9.5mm equivalent stress

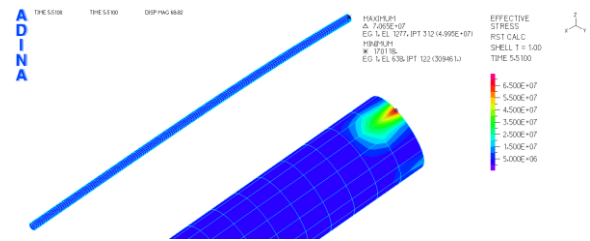


Fig.3 Wall thickness is 16.9mm equivalent stress

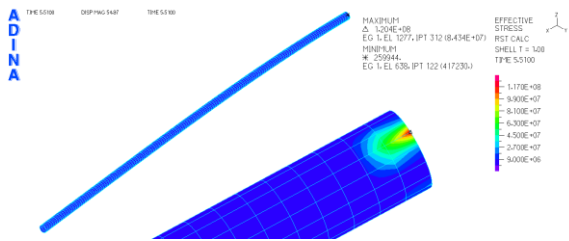


Fig.4 Wall thickness is 16.9mm equivalent stress

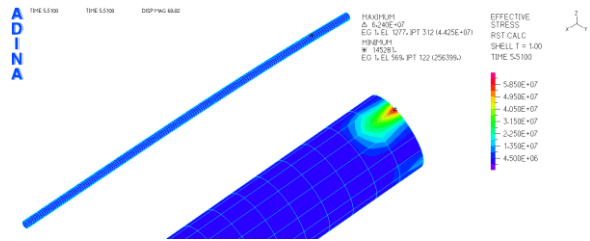


Fig.5 Wall thickness is 28.7mm equivalent stress

We can see from Figure 2 to Figure 5, in the case of different thickness, the stress changes of the entire pipe are relatively small, the stress changes mainly in the pipeline near the junction, the upper end of the pipe connection at the maximum stress occurs.

Fitting the different thickness of the point of maximum stress, as the corresponding curve shown in Figure 3. The law of maximum stress value with thickness variation as follow.

$$y = 2.111 \times 10^{11} x^2 - 1.18 \times 10^{10} x + 2 \times 10^8 \quad (16)$$

We can see from the curves shown in Figure 6, with the Support pipe wall thickness increases, the maximum stress decreases. From the diagram, we can calculate each increase the thickness of 2.4mm, the maximum stress value decreased 19.3%, 15.9%, 13.5%, 11.7%, 10.3%, 9.2%, 8.3%, 7.6%, and the thickness of 28.7mm reduced 64.2% than 9.5mm. From these data, the stress reducing effect can be found by increasing the wall thickness so that increasingly smaller.

Fitting the different thickness of the point of minimum stress, as the corresponding curve shown in Figure 5. The law of minimum stress value with thickness variation as follow.

$$y = 33282 \times 10^4 x^2 - 22208 \times 10^3 x + 435540 \quad (17)$$

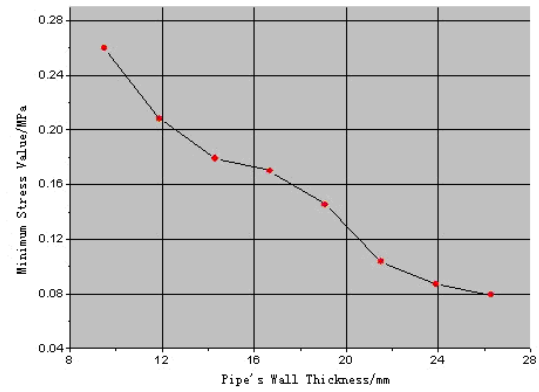
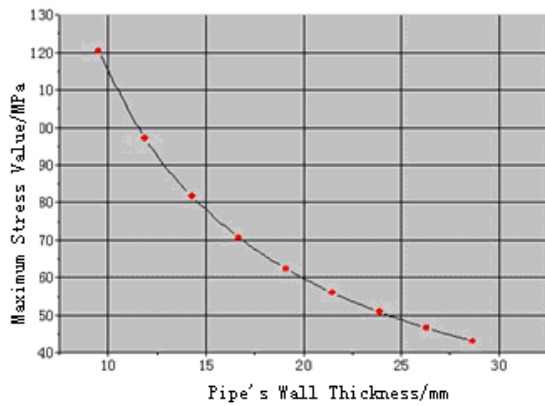


Fig.6 Maximum stress of different wall thickness Fig.7 Minimum stress of different wall thickness

We can see from the curves shown in Figure 7, with the pipe wall thickness increases, the minimum stress decreases. From the diagram, we can calculate each increase the thickness of 2.4mm, the minimum stress value decreased 19.9%, 14.0%, 5%, 14.6%, 28.7%, 15.9%, 8.6%, 2.7%, and the thickness of 28.7mm reduced 70.2% than 9.5mm. From these data, the stress reducing effect can be found by increasing the wall thickness so that increasingly smaller.

Conclusion

By studying mining institutions with the bracket connected, the pipeline was impacted by the external flow velocity of 1.8m / s, the internal conveying speed is 2 m / s, We obtained the law of effects such as stress and some meaningful conclusions as the follows.

- 1) In the case of different thickness, the stress changes of the entire pipeline is relatively small, it is mainly in the pipes close to the junction, the maximum stress occurs at the upper end of the pipe connection.
- 2) With the Support pipe wall thickness increases, the maximum stress decreases. From the diagram, we can calculate each increases the thickness of 2.4mm, the maximum stress value decreased 19.3%, 15.9%, 13.5%, 11.7%, 10.3%, 9.2%, 8.3%, 7.6%, and the thickness of 28.7mm reduced 64.2% than 9.5mm. From these data, the stress reducing effect can be found by increasing the wall thickness so that increasingly smaller.
- 3) With the support pipe wall thickness increases, the minimum stress value decreases. From the diagram, we can calculate each increases the thickness of 2.4mm, the minimum stress value decreased 19.9%, 14.0%, 5%, 14.6%, 28.7%, 15.9%, 8.6%, 2.7%, and the thickness of

28.7mm reduced 64.2% than 9.5mm. From these data, the stress reducing effect can be found by increasing the wall thickness so that increasingly smaller.

Acknowledgements

This project is supported by China National Natural Science Foundation of China (51174087)

References

- [1] M. Heil (2004). "An efficient solver for the fully coupled solution of large- displacement fluid-structure interaction problems". *Computer Methods in Applied Mechanics and Engineering* 193: 1–23.
- [2] K.-J. Bathe; H. Zhang (2004). "Finite element developments for general fluid flows with structural interactions". *International Journal for Numerical Methods in Engineering* 60: 213–232.
- [3] J. Hron, S. Turek (2006). A monolithic FEM/multigrid solver for ALE formulation of fluid-structure interaction with application in biomechanics. *Lecture Notes in Computational Science and Engineering. Fluid–Structure Interaction – Modelling, Simulation, Optimisation*. Springer-Verlag. pp. 146–170.
- [4] J. Degroote, K.-J. Bathe, J. Vierendeels (2009). "Performance of a new partitioned procedure versus a monolithic procedure in fluid–structure interaction". *Computers and Structures* 87: 793.
- [5] J. Vierendeels, L. Lanoye, J. Degroote, P. Verdonck (2007). "Implicit coupling of partitioned fluid-structure interaction problems with reduced order models". *Computers and Structures* 85 (11–14): 970–976.
- [6] U. Küttler, W. Wall (2008). "Fixed-point fluid-structure interaction solvers with dynamic relaxation". *Computational Mechanics* 43 (1): 61–72.
- [7] J. Degroote, P. Bruggeman, R. Haelterman, J. Vierendeels (2008). "Stability of a coupling technique for partitioned solvers in FSI applications". *Computers and Structures* 86 (23–24): 2224–2234.
- [8] R. Jaiman, X. Jiao, P. Geubelle, E. Loth (2006). "Conservative load transfer along curved fluid-solid interface with non-matching meshes". *Journal of Computational Physics* 218 (1): 372–397.

- [9] J. Vierendeels, K. Dumont, E. Dick, P. Verdonck (2005). "Analysis and stabilization of fluid-structure interaction algorithm for rigid-body motion". *AIAA Journal* 43 (12): 2549–2557.
- [10] J. Vierendeels, L. Lanoye, J. Degroote, P. Verdonck (2007). "Implicit coupling of partitioned fluid-structure interaction problems with reduced order models". *Computers and Structures* 85 (11–14): 970–976.
- [11] U. Küttler, W. Wall (2008). "Fixed-point fluid-structure interaction solvers with dynamic relaxation". *Computational Mechanics* 43 (1): 61–72.
- [12] J. Degroote, P. Bruggeman, R. Haelterman, J. Vierendeels (2008). "Stability of a coupling technique for partitioned solvers in FSI applications". *Computers and Structures* 86 (23–24): 2224–2234.
- [13] ZHANG Zhi-ping, HUANG Wei-ping, LI Hua-jun, The nonlinear dynamic analysis of offshore platform structure in case of considering the fluid-structure interaction [J], *Periodical of Ocean University of China*, 2005,35 (5) : 823-826
- [14] Mr Yang, Fan Shi-Juan, Pipes for Fluid coupled vibration numerical analysis[J]. *Vibration and Shock*, 2009,28(6):2148-2157.
- [15] YUE Ga, The advanced applications of ADINA fluid and fluid-structure interaction [M]. Beijing: The China Communication Press, 2010